

Explicit equations for two-dimensional water waves with constant vorticity

V. P. Ruban*

Landau Institute for Theoretical Physics, 2 Kosygin Street, 119334 Moscow, Russia

(Dated: October 26, 2018)

Governing equations for two-dimensional inviscid free-surface flows with constant vorticity over arbitrary non-uniform bottom profile are presented in exact and compact form using conformal variables. An efficient and very accurate numerical method for this problem is developed.

PACS numbers: 47.15.ki, 47.35.-i, 47.10.-g, 47.11.-j

Most theories for surface water waves have been developed under assumption of irrotational flows (see, for example, Refs.[1–3], and references therein). The reason is that irrotational incompressible flows are completely determined by the boundary distribution of the velocity potential through solution of the Laplace equation, and this fact effectively reduces spatial dimensionality of the problem. However, in many real situations waves propagate on shear currents, and over non-uniform depth. Interaction between waves and currents is important in many aspects, for example, as a mechanism of giant wave formation [4–6]. The fully nonlinear problem of vortical flows under free surface is very complicated. Various simplifications are assumed in theoretical studies, as weak nonlinearity, mild slope, long wave length, and so on (see, for examples, Refs.[7–12]). The only possibility for non-potential flows, when dimensionality is reduced, is the two-dimensional (2D) problem with constant vorticity, since in this case all perturbations are irrotational. In particular, relatively long solitary waves in water of finite uniform depth with constant vorticity were calculated analytically [13, 14]. There are also fully nonlinear numerical results for steady flows obtained by a boundary integral method (see Refs.[15–17], and references therein). At the same time, unsteady rotational waves have not been extensively simulated. The present work is intended to fill this gap. Here for the first time an exact and compact formulation of the fully nonlinear problem of waves with constant vorticity is presented in terms of so called conformal variables. The conformal variables were introduced earlier and successfully used to describe purely potential flows on a constant depth or on infinitely deep water [18–22]. Later, the description has been generalized by the present author to the case of potential flows over arbitrary non-uniform and time-dependent bottom profile [23, 24]. One of the main advantages of equations in conformal variables is an easy numerical implementation with fast Fourier transform (FFT) subroutines. In this work, after derivation of exact evolutionary equations, some illustrative numerical results will be presented. Here, for simplicity, a non-uniform bottom profile does not depend on time, though a generalization to non-static bottom is straightforward.

Derivation of exact equations. In what follows, style and notations will be the same as in Ref.[24]. We consider here a 2D incompressible inviscid non-stationary flow in (x, y) -plane, bounded by a given bottom profile from below and by an unknown free surface from above. The flow is rotational, with a constant vorticity field, $\partial_x V_{(y)} - \partial_y V_{(x)} = -\Omega = const$. The velocity field thus can be represented as follows, $\mathbf{V} = (\Omega y + \varphi_x, \varphi_y)$, where the potential $\varphi(x, y, t)$ satisfies the Laplace equation $\varphi_{xx} + \varphi_{yy} = 0$. Let us also introduce a harmonically conjugate function $\theta(x, y, t)$: $\varphi_x = \theta_y, \varphi_y = -\theta_x$. Then it is easy to check that two components of the vector Euler equation are equivalent to a single scalar equation, analogous to the Bernoulli equation,

$$\varphi_t - \Omega\theta + \Omega y \varphi_x + (\varphi_x^2 + \varphi_y^2)/2 + gy + p/\rho_* = const, \quad (1)$$

where g is the gravity acceleration, ρ_* is a constant density of the fluid, and $p(x, y, t)$ is the pressure. It is Eq.(1) that makes possible reduction of dimensionality of the problem, in the same manner as for purely potential flows.

Important point is that complex combination $\tilde{\phi}(z, t) = \varphi(x, y, t) + i\theta(x, y, t)$ is an analytic function of the complex argument $z = x + iy$. Analyticity is preserved under conformal coordinate transforms $z = z(w, t)$, where $w = u + iv$ is a new complex variable. We choose an analytic function $z(w, t)$ in such a manner that $w = u$ at the bottom and $w = u + i$ at the free surface. Shape of the surface will be given in a parametric form,

$$X^{(s)}(u, t) + iY^{(s)}(u, t) \equiv Z^{(s)}(u, t) = z(u + i, t), \quad (2)$$

The bottom profile will be determined by

$$X^{(b)}(u, t) + iY^{(b)}(u, t) \equiv Z^{(b)}(u, t) = z(u, t). \quad (3)$$

Thus, we have an analytic function $\phi(w, t) = \tilde{\phi}(z(w, t), t)$ defined in the stripe $0 \leq v \leq 1$ in the (u, v) -plane. Let us designate boundary values of this function as written below,

$$\phi(u + i, t) \equiv \Phi^{(s)}(u, t), \quad \phi(u, t) \equiv \Phi^{(b)}(u, t). \quad (4)$$

Since $\Phi^{(s)}(u, t)$ and $\Phi^{(b)}(u, t)$ are values of the same analytic function at points u and $u + i$, they are related to each other by a linear transform (see [24]),

$$\Phi^{(s)}(u, t) = e^{-\hat{k}} \Phi^{(b)}(u, t), \quad (5)$$

*Electronic address: ruban@itp.ac.ru

with $e^{-\hat{k}} \equiv \exp(i\hat{\partial}_u)$. That means $\Phi_k^{(s)}(t) = e^{-k}\Phi_k^{(b)}(t)$ for the corresponding Fourier images.

The velocity components are determined by the following relations

$$\begin{aligned} V_{(x)} - iV_{(y)} &= \Omega y + \varphi_x - i\varphi_y = \Omega \text{Im}z + d\tilde{\phi}/dz \\ &= \Omega \text{Im}z(w, t) + \phi'(w, t)/z'(w, t). \end{aligned} \quad (6)$$

Now we are going to write equations of motion in the conformal variables. First, we have two kinematic conditions which in our case take form

$$-\text{Im} \left(Z_t^{(s)} \bar{Z}_u^{(s)} \right) = [\text{Im} \Phi^{(s)} + (\Omega/2)(\text{Im} Z^{(s)})^2]_u, \quad (7)$$

$$0 = [\text{Im} \Phi^{(b)} + (\Omega/2)(\text{Im} Z^{(b)})^2]_u, \quad (8)$$

where \bar{Z} denotes complex conjugate value, and the subscripts denote the corresponding partial derivatives. At free surface the pressure is constant (we neglect here surface tension σ , otherwise $p^{(s)} = \sigma\kappa + \text{const}$, where κ is the surface curvature). Therefore from Eq.(1) we have the dynamic boundary condition in conformal variables,

$$\begin{aligned} \text{Re} \left(\Phi_t^{(s)} - \Phi_u^{(s)} Z_t^{(s)} / Z_u^{(s)} \right) + |\Phi_u^{(s)} / Z_u^{(s)}|^2 / 2 + g \text{Im} Z^{(s)} \\ - \Omega \text{Im} \Phi^{(s)} + \Omega \text{Im} Z^{(s)} \text{Re} \left(\Phi_u^{(s)} / Z_u^{(s)} \right) = 0. \end{aligned} \quad (9)$$

Taking into account Eq.(8), it is convenient to represent $\Phi^{(b)}(u, t)$ in the form

$$\Phi^{(b)} = \hat{S}\psi - i(\Omega/2)(1 - i\hat{R})[Y^{(b)}]^2, \quad (10)$$

where $\psi(u, t)$ is some unknown real function, and the linear operators \hat{S} and \hat{R} are diagonal in Fourier representation: $S_k = 1/\cosh(k)$, $R_k = i \tanh(k)$. It is essential that when \hat{S} or \hat{R} acts on a purely real function, the result is also real. We will also need operator $T_k = -i \coth(k) = R_k^{-1}$. Since $e^{-\hat{k}}\hat{S} = (1 + i\hat{R})$ and $e^{-\hat{k}}(1 - i\hat{R}) = \hat{S}$, we have from Eqs.(5) and (10) the following formula for $\Phi^{(s)}(u, t)$,

$$\Phi^{(s)} = (1 + i\hat{R})\psi - i(\Omega/2)\hat{S}[Y^{(b)}]^2. \quad (11)$$

Now we should take into account that the function $z(w, t)$ can be represented as a composition of two functions (see [23, 24]), that is $z(w, t) = Z(\zeta(w, t))$, where a known analytic function $Z(\zeta) = X(\zeta) + iY(\zeta)$ determines bottom shape. The conformal mapping $Z(\zeta)$ does not have any singularities within a sufficiently wide horizontal stripe above the real axis in ζ -plane. An intermediate analytic function $\zeta(w, t)$ takes real values at the real axis, and therefore

$$\zeta(w, t) = \int \frac{a_k(t)}{\cosh(k)} e^{ikw} \frac{dk}{2\pi}, \quad a_{-k} = \bar{a}_k, \quad (12)$$

where $a_k(t)$ is Fourier transform of a real function $a(u, t)$. On the bottom $\zeta(u, t) = \hat{S}a(u, t)$, therefore

$$Z^{(b)}(u, t) = Z(\hat{S}a(u, t)), \quad (13)$$

At the free surface we have relations

$$\zeta(u + i, t) \equiv \xi(u, t) = (1 + i\hat{R})a(u, t), \quad (14)$$

and $Z^{(s)} = Z(\xi)$, $Z_u^{(s)} = Z_\xi(\xi)\xi_u$, $Z_t^{(s)} = Z_\xi(\xi)\xi_t$.

Thus we have in our system two unknown real functions, $\psi(u, t)$ and $a(u, t)$. All the other quantities are expressed through these two. Our purpose now is to derive equations determining time derivatives ψ_t and a_t . To do this, we divide Eq.(7) by $|Z_u^{(s)}|^2$ and obtain that $\text{Im}(\xi_t/\xi_u) = -Q$, where

$$Q \equiv \frac{\{\hat{R}\psi + (\Omega/2)([\text{Im} Z(\xi)]^2 - \hat{S}[\text{Im} Z(\hat{S}a)]^2)\}_u}{|Z_\xi(\xi)\xi_u|^2}. \quad (15)$$

Since $\xi_t/\xi_u = \zeta_t(w, t)/\zeta_w(w, t)|_{w=u+i}$, there exists a relation between the real and imaginary parts: $\text{Im}(\xi_t/\xi_u) = \hat{R} \text{Re}(\xi_t/\xi_u)$, so $\text{Im}(\xi_t/\xi_u) = -Q$ means $\xi_t = -\xi_u(\hat{T} + i)Q$ and it gives us equation determining a_t ,

$$a_t = -\text{Re}[\xi_u(\hat{T} + i)Q]. \quad (16)$$

After that, Eqs.(9) and (11) allow us to express ψ_t :

$$\begin{aligned} \psi_t &= -\text{Re}[\Phi_u^{(s)}(\hat{T} + i)Q] - |\Phi_u^{(s)} / Z_u^{(s)}|^2 / 2 - g \text{Im} Z^{(s)} \\ &+ \Omega \text{Im} \Phi^{(s)} - \Omega \text{Im} Z^{(s)} \text{Re} \left(\Phi_u^{(s)} / Z_u^{(s)} \right). \end{aligned} \quad (17)$$

Now, exact and explicit evolutionary equations have been derived. In the next section it is explained how one can numerically simulate them with a high accuracy.

Numerical method and example. Let us consider the case when a bottom profile is periodic on x . Obviously, there exist solutions with velocity field and surface elevation having the same spatial period L . Without loss of generality, the potential $\varphi(x, y, t)$ can be assumed periodic (the part of φ which is proportional to x and corresponds to a constant horizontal velocity, can be excluded by a redefinition of y zero level). Making a proper choice for the length and time scales, we may write $g = 1$, and $Z(\zeta + 2\pi) = 2\pi + Z(\zeta)$. Direct substitution into Eqs.(16) and (17) shows the solutions are 2π -periodic on the variable $\vartheta = u\alpha(t)$, where a real function $\alpha(t)$ depends on time in a non-trivial manner in order to cancel non-periodic terms in Eqs.(16) and (17). The non-periodic terms take place because the operator \hat{T} is singular at small k , and its action on a constant function Q_0 is non-periodic: $\hat{T}Q_0 = Q_0u$ (see Refs.[23, 24]). So, we can write for rescaled dimensionless quantities

$$a(\vartheta, t) = \vartheta + \sum_{m=-\infty}^{+\infty} \rho_m(t) \exp(im\vartheta), \quad (18)$$

$$\xi(\vartheta, t) = \vartheta + i\alpha(t) + \sum_{m=-\infty}^{+\infty} \frac{2\rho_m(t) \exp(im\vartheta)}{1 + \exp(2m\alpha(t))}, \quad (19)$$

$$\psi(\vartheta, t) = \sum_{m=-\infty}^{+\infty} \psi_m(t) \exp(im\vartheta), \quad (20)$$

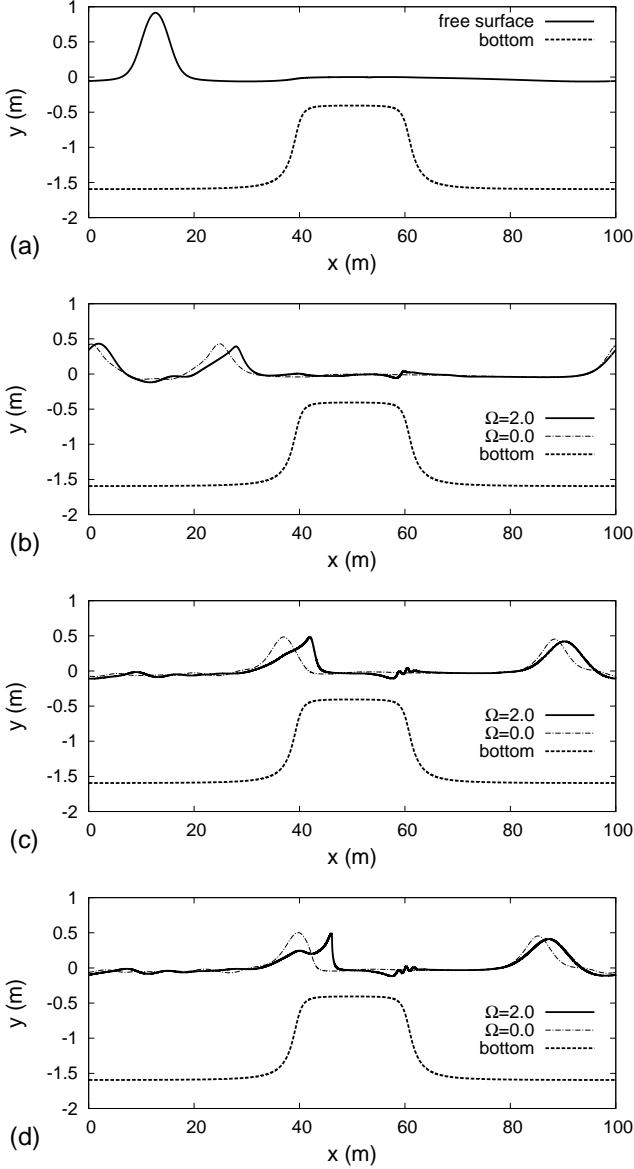


FIG. 1: Shape of the free surface at different time moments; a) $t = 0.00$ s; b) $t = 2.8$ s; c) $t = 5.6$ s, d) $t = 6.32$ s.

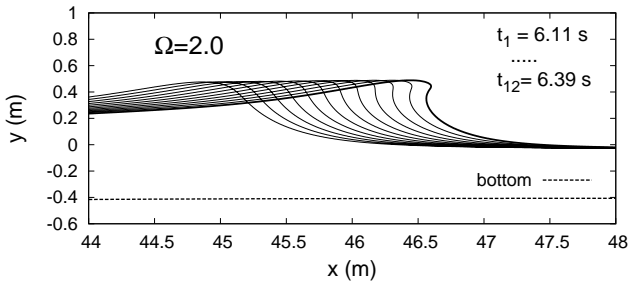


FIG. 2: Profiles of the overturning wave from $t = 6.11$ s (left curve) to $t = 6.39$ s (right curve).

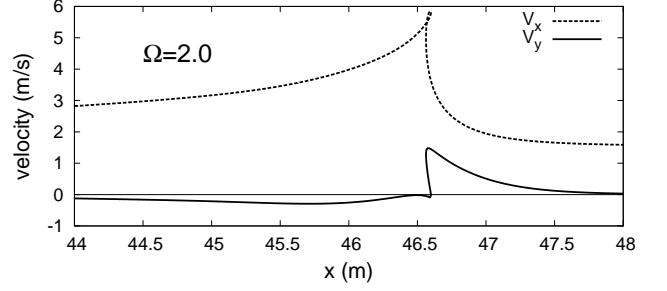


FIG. 3: Velocity distribution at the free surface for $t = 6.39$ s.

where $\rho_m(t)$ and $\psi_m(t)$ are Fourier coefficients of 2π -periodic real functions $\rho(\vartheta, t)$ and $\psi(\vartheta, t)$. As a result, in variables (ϑ, t) equations for ρ_t and ψ_t look similar to Eqs.(16) and (17), but all the u -derivatives should be replaced by ϑ -derivatives, and operators \hat{R} , \hat{S} , and \hat{T} should be everywhere replaced by new operators \hat{R}_α , \hat{S}_α , and \hat{T}_α respectively:

$$\rho_t = -\text{Re}[\xi_\vartheta(\hat{T}_\alpha + i)\mathbf{Q}], \quad (21)$$

$$\begin{aligned} \psi_t = & -\text{Re}[\Phi_\vartheta(\hat{T}_\alpha + i)\mathbf{Q}] - \frac{|\Phi_\vartheta|^2}{2|Z_\xi(\xi)\xi_\vartheta|^2} - g \text{Im} Z(\xi) \\ & + \Omega \text{Im} \Phi - \Omega \text{Im} Z(\xi) \text{Re} \left(\frac{\Phi_\vartheta}{Z_\xi(\xi)\xi_\vartheta} \right), \end{aligned} \quad (22)$$

where $\xi = \vartheta + i\alpha + (1 + i\hat{R}_\alpha)\rho$, and

$$\Phi = (1 + i\hat{R}_\alpha)\psi - i(\Omega/2)\hat{S}_\alpha Y^2(\vartheta + \hat{S}_\alpha\rho), \quad (23)$$

$$\mathbf{Q} = \frac{\{\hat{R}_\alpha\psi + (\Omega/2)[Y^2(\xi) - \hat{S}_\alpha Y^2(\vartheta + \hat{S}_\alpha\rho)]\}_\vartheta}{|Z_\xi(\xi)\xi_\vartheta|^2}. \quad (24)$$

These new operators are diagonal in the discrete Fourier representation: $\mathbf{R}_\alpha(m) = i \tanh(\alpha m)$, $\mathbf{S}_\alpha(m) = 1/\cosh(\alpha m)$, and $\mathbf{T}_\alpha(m) = -i \coth(\alpha m)$ for $m \neq 0$, $\mathbf{T}_\alpha(0) = 0$. The system of equations is closed by the following condition for $\dot{\alpha}(t)$, which ensures cancellation of the non-periodic terms in Eqs.(16) and (17),

$$\dot{\alpha}(t) = -\frac{1}{2\pi} \int_0^{2\pi} \mathbf{Q}(\vartheta) d\vartheta. \quad (25)$$

The above system of equations has two apparent integrals of motion, namely the area A occupied by fluid, $A = A_0 + \int Y(\xi) \text{Re}[Z_\xi(\xi)\xi_\vartheta] d\vartheta$, and the total energy E (kinetic energy plus potential energy in the gravitational field),

$$\begin{aligned} E = & E_0 + \frac{\Omega^2}{6} \int Y^3(\xi) \text{Re}[Z_\xi(\xi)\xi_\vartheta] d\vartheta \\ & + \frac{\Omega^2}{8} \int Y^2(\vartheta + \hat{S}_\alpha\rho) \hat{R}_\alpha[Y^2(\vartheta + \hat{S}_\alpha\rho)]_\vartheta d\vartheta \\ & + \frac{\Omega}{2} \int [Y^2(\xi) - \hat{S}_\alpha Y^2(\vartheta + \hat{S}_\alpha\rho)] \psi_\vartheta d\vartheta \\ & - \frac{1}{2} \int \psi \hat{R}_\alpha \psi_\vartheta d\vartheta + \frac{g}{2} \int Y^2(\xi) \text{Re}[Z_\xi(\xi)\xi_\vartheta] d\vartheta, \end{aligned} \quad (26)$$

where A_0 and E_0 are constant, and all the integrals are in the limits from 0 to 2π .

Eqs.(21)-(25) are easy for numerical simulation if the function $Z(\zeta)$ is given by a simple formula as it takes place for many interesting bottom profiles. The numerical method employed here is naturally based on the discrete Fourier representation, since all the linear operators in the equations are efficiently computed with modern FFT subroutines in m -representation, while all the nonlinear operations are simple in ϑ -representation. As primary dynamical variables, the quantities $\alpha(t)$, $\rho_m(t)$, and $\psi_m(t)$ are taken, with $0 \leq m < M$ (for negative m the relations $\rho_{-m} = \bar{\rho}_m$ and $\psi_{-m} = \bar{\psi}_m$ are used). After each step of a Runge-Kutta 4-th order procedure, only spectral components with $|m| < M_{eff}$ are kept, where $M_{eff} \approx (1/4)N$, $M \approx (3/8)N$, and $N = 2^{12\dots 19}$ is the size of arrays for the fast Fourier transform (during computations, N is doubled several times as small-scale structures develop). As a result of the adaptive increasing of N , the right hand sides of Eqs.(21)-(22) can be computed with nearly the same numerical error $\delta_0 < N10^{-18}$ as it is for the FFT subroutine using C-type `double`. Since the time step is decreased as $\tau \sim 1/N$ for the stability reasons, an error for the free surface position at $t \sim 1$ can be estimated as $\delta \lesssim N^2 10^{-18}$. Practically, A and E are conserved up to 10 decimal digits for most part of the evolution. In a final stage, the larger N_{final} is used, the later time moment is when the high accuracy is lost.

Here an example is given which demonstrates potentialities of the method. Let the bottom profile be determined by formula $Z(\zeta) = iY_0 + \mathcal{B}(\zeta - i\alpha_0)$, where $Y_0 = 0.02\pi$, $\alpha_0 = 0.02\pi$, and

$$\mathcal{B}(q) = q - i\Delta \text{Ln} \left[\left(i \sin q + \sqrt{\epsilon + \cos^2 q} \right) (1 + \epsilon)^{-1/2} \right],$$

with $\Delta = 0.6$ and $\epsilon = 0.02$. At $t = 0$ we put $\alpha = \alpha_0$ and $\rho = 0.05 \tanh[15 \sin(\vartheta - \gamma)] \exp[-2(1 - \cos(\vartheta - \gamma))]$, where

$\gamma = 0.5$. In Fig.1-a, the bottom profile and the initial surface shape are presented normalized to the spatial period $L = 100$ m and shifted appropriately in the vertical direction. Dimensionless vorticity $\Omega = 2.0$ together with the parameter Y_0 give the rotational part of the horizontal velocity field $V_{(x)}^{(\Omega)} \approx 1.6(y+1)$ m/s. This corresponds to a backward flow along the bottom in the deeper regions. We choose $\psi(\vartheta, 0)$ in such a way that at $t = 0$ the normal component of the total velocity field at the free surface is zero: $\psi(\vartheta, 0) = -(\Omega/2)\hat{T}_\alpha[Y^2(\xi) - \hat{S}_\alpha Y^2(\vartheta + \hat{S}_\alpha \rho)]$. Some results of the computation are presented in Fig.1, where also a comparison is made to the case $\Omega = 0$. The initial hump at the surface decays into two oppositely propagating solitary waves having different speeds and different profiles (crest of the right-propagating wave is more sharp; however, a maximum curvature is finite). In this example the right-propagating wave first meets the region of relatively shallow depth, where its crest becomes more and more steep, and finally the wave profile overturns, as it is seen in Fig.2. Velocity distribution along the overturning wave is shown in Fig.3. Another interesting phenomenon observed here is the wave blocking near $x \approx 60$ m, where an average horizontal flow velocity (~ 1.6 m/s for $\Omega = 2.0$) approaches speed of typical waves $v_{ph} \approx \sqrt{gh}$ (h is the local depth), and therefore waves cannot enter the shallow region from the right. In different simulations, for $\Omega \gtrsim 2.4$, the blocking was so strong that wave height near the point $x = 60$ was comparable to the local depth (not shown). However, an extensive discussion of this phenomenon is not possible in this Brief Report.

Acknowledgments. These investigations were supported by RFBR Grant 06-01-00665, by the Program ‘‘Fundamental Problems of Nonlinear Dynamics’’ from the RAS Presidium, and by Grant ‘‘Leading Scientific Schools of Russia’’.

-
- [1] V.E. Zakharov, Sov. Phys. JETP **24**, 455 (1967).
 [2] V. E. Zakharov, Eur. J. Mech. B/Fluids **18**, 327 (1999).
 [3] P. M. Lushnikov and V. E. Zakharov, Physica D **203**, 9 (2005).
 [4] D.H. Peregrine, Adv. Appl. Mech. **16**, 9 (1976).
 [5] C. Kharif and E. Pelinovsky, Eur. J. Mech. B/Fluids **22**, 603 (2003).
 [6] I.V. Lavrenov and A.V. Porubov, Eur. J. Mech. B/Fluids **25**, 574 (2006).
 [7] T.B. Benjamin, J. Fluid Mech. **12**, 97 (1962).
 [8] N.C. Freeman and R.S. Johnson, J. Fluid Mech. **42**, 401 (1970).
 [9] C.S. Yih, J. Fluid Mech. **51**, 209 (1972).
 [10] R.S. Johnson, J. Fluid Mech. **215**, 145 (1990).
 [11] <http://chinacat.coastal.udel.edu/~kirby/>
 [12] K.A. Belibassakis, J. Fluid Mech. **578**, 413 (2007).
 [13] V. A. Miroshnikov, J. Fluid Mech. **456**, 1 (2002).
 [14] W. Choi, Phys. Rev. E **68**, 026305 (2003).
 [15] A.F. Teles da Silva and D. H. Peregrine, J. Fluid Mech. **195**, 281 (1988).
 [16] D. I. Pullin and R. H. J. Grimshaw, Phys Fluids **31**, 3550 (1988).
 [17] J.-M. Vanden-Broeck, J. Fluid Mech. **274**, 339 (1994); J.-M. Vanden-Broeck, Eur. J. Mech. B/Fluids **14**, 761 (1995); J.-M. Vanden-Broeck, IMA J. Appl. Math. **56**, 207 (1996).
 [18] A. I. Dyachenko *et al.*, Phys. Lett. A **221**, 73 (1996).
 [19] A. I. Dyachenko, V. E. Zakharov, and E. A. Kuznetsov, Fiz. Plazmy **22**, 916 (1996) [Plasma Phys. Rep. **22**, 829 (1996)].
 [20] V. E. Zakharov, A. I. Dyachenko, and O. A. Vasilyev, Eur. J. Mech. B/Fluids **21**, 283 (2002).
 [21] A. I. Dyachenko and V. E. Zakharov, Pis'ma v ZhETF **81**, 318 (2005) [JETP Letters **81**, 255 (2005)].
 [22] V.E. Zakharov, A.I. Dyachenko and A.O. Prokofiev, Eur. J. Mech. B/Fluids **25**, 677 (2006).
 [23] V. P. Ruban, Phys. Rev. E **70**, 066302 (2004).
 [24] V. P. Ruban, Phys. Lett. A **340**, 194 (2005).